

QCD in the heavy dense regime: Large N_c and quarkyonic matter*

OWE PHILIPSEN[†], JONAS SCHEUNERT

ITP, Goethe-Universität Frankfurt
Max-von-Laue-Str.1
60438 Frankfurt am Main, Germany

After combined character and hopping expansions and integration over the spatial gauge links, lattice QCD reduces to a three-dimensional $SU(3)$ Polyakov loop model with complicated interactions. A simple truncation of the effective theory is valid for heavy quarks on reasonably fine lattices and can be solved by linked cluster expansion in its effective couplings. This was used earlier to demonstrate the onset transition to baryon matter in the cold and dense regime. Repeating these studies for general N_c , one finds that for large N_c the onset transition becomes first-order, and the pressure scales as $p \sim N_c$ through three consecutive orders in the hopping expansion. These features are consistent with the formal definition of quarkyonic matter given in the literature. We discuss the implications for $N_c = 3$ and physical QCD.

1. Introduction

The physics of cold and dense baryon matter is of ever increasing interest in view of growing observational data from neutron stars and their mergers, as well as heavy-ion collisions at low energies and large densities. To date, the corresponding parametric regime of QCD is inaccessible to lattice simulations because of a severe sign problem for baryo-chemical potential $\mu_B \neq 0$. The low density regime $\mu_B < 3T$, where the crossover from a hadron resonance gas to a quark gluon plasma takes place, can be controlled by a number of methods, and no sign of criticality is observed [1, 2]. Here we address the cold and dense regime of the nuclear liquid gas transition, corresponding to large μ_B/T , within an effective lattice theory derived analytically from full QCD. While this theory is only valid for heavy quarks, the qualitative features of the nuclear liquid gas transition can be

* Presented at ‘Criticality in QCD and the hadron resonance gas’, Wroclaw, July 29-31, 2020

[†] Speaker

reproduced directly from QCD in this framework. In particular, we discuss here the possibility for quarkyonic matter as conjectured in [3].

2. An effective lattice theory for heavy quarks

We start with lattice QCD in the Wilson fomulation at finite temperature, i.e., with compact euclidean time dimension of N_τ slices, $T = 1/(aN_\tau)$, and (anti-)periodic boundary conditions for (fermions) bosons. An effective theory in terms of temporal links only is obtained after integrating over the quark fields and gauge links in spatial directions in the partition function,

$$Z = \int DU_0 DU_i \det Q e^{-S_g[U]} \equiv \int DU_0 e^{-S_{eff}[U_0]} = \int DW e^{-S_{eff}[W]} . \quad (1)$$

The effective action then depends on temporal Wilson lines $W(\mathbf{x})$ closing through the periodic boundary, or Polyakov loops $L(\mathbf{x}) = \text{Tr}W(\mathbf{x})$, and is in principle unique and exact. In practice, we first expand the QCD action in powers of the coefficient of the fundamental character u and the hopping parameter κ ,

$$u(\beta) = \frac{\beta}{18} + \frac{\beta^2}{216} + \dots < 1, \quad \kappa = \frac{1}{2am_q + 8} . \quad (2)$$

The dependence of u on the lattice gauge coupling $\beta = 2N_c/g^2$ is known to arbitrary precision, and u is always smaller than one for finite β -values. Since the hopping expansion is in inverse quark mass, the effective theory to low orders is valid for heavy quarks only. Both expansions result in convergent series within a finite radius of convergence. Truncating these at some finite order, the integration over the spatial gauge links can be performed analytically to provide a closed expression for the effective theory. The integration over spatial links causes long-range interactions of Polyakov loops at all distances and to all powers, which must be taken into account according to the power counting of the expansion parameters. The first terms of the partition function, with nearest neighbour interactions only, then read [4, 5]

$$\begin{aligned} Z = & \int DW \prod_{\langle \mathbf{x}, \mathbf{y} \rangle} [1 + \lambda(L_{\mathbf{x}}L_{\mathbf{y}}^* + L_{\mathbf{x}}^*L_{\mathbf{y}})] \quad (3) \\ & \times \prod_{\mathbf{x}} [1 + h_1 L_{\mathbf{x}} + h_1^2 L_{\mathbf{x}}^* + h_1^3]^{2N_f} [1 + \bar{h}_1 L_{\mathbf{x}}^* + \bar{h}_1^2 L_{\mathbf{x}} + \bar{h}_1^3]^{2N_f} \prod_{\langle \mathbf{x}, \mathbf{y} \rangle} \left(1 - \right. \\ & \left. 2h_2 \left(\text{Tr} \frac{h_1 W_{\mathbf{x}}}{1 + h_1 W_{\mathbf{x}}} - \text{Tr} \frac{\bar{h}_1 W_{\mathbf{x}}^\dagger}{1 + \bar{h}_1 W_{\mathbf{x}}^\dagger} \right) \left(\text{Tr} \frac{h_1 W_{\mathbf{y}}}{1 + h_1 W_{\mathbf{y}}} - \text{Tr} \frac{\bar{h}_1 W_{\mathbf{y}}^\dagger}{1 + \bar{h}_1 W_{\mathbf{y}}^\dagger} \right) \right) . \end{aligned}$$

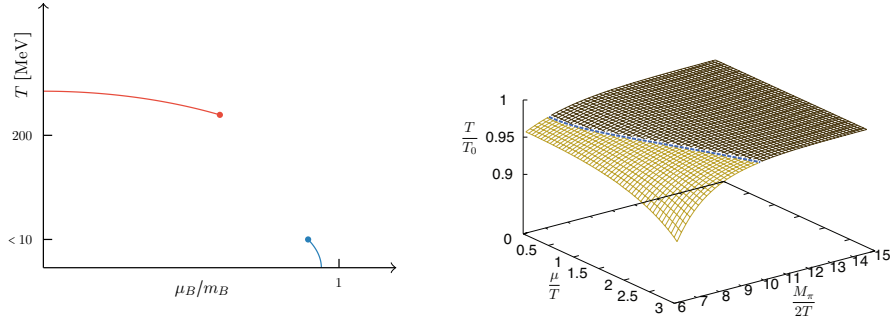


Fig. 1. Left: Qualitative phase diagram for QCD with very heavy quarks. Right: Deconfinement transition for $N_f = 2$, $N_\tau = 6$ from the 3d effective theory [5].

The first line corresponds to the Yang-Mills part, the second line to the static determinant, and the third line to the leading corrections from quark hops representing pion exchange. The effective couplings are functions of the original QCD parameters (for complete expressions beyond LO, see [5])

$$\begin{aligned}
 \lambda &= u^{N_\tau} \exp[N_\tau(4u^4 + \dots)] , \\
 h_1 &= (2\kappa e^{a\mu})^{N_\tau} (1 + \dots) = e^{\frac{\mu - m}{T}} (1 + \dots), \quad \bar{h}_1 = h_1(-\mu) , \\
 h_2 &= \kappa^2 N_\tau / N_c (1 + \dots) .
 \end{aligned} \tag{4}$$

with $am = -\ln(2\kappa) = am_B/3$ the leading-order constituent quark mass in a baryon.

This effective theory has a mild sign problem only and can be simulated with reweighting or complex Langevin methods [5, 6]. Moreover, it can be treated by linked-cluster expansion methods known from statistical physics. These have recently been tested to high order in an $SU(3)$ spin model, allowing a quantitative determination of the phase diagram with zero or non-zero chemical potential [7]. Also in the present context, a linked cluster expansion to order $\kappa^8 u^5$ was successfully tested against numerical ones [8].

2.1. The deconfinement transition

The effective theory can now be used to map out the phase diagram of QCD with heavy quarks. At $\mu = 0$ and infinite quark mass, a first-order deconfinement transition is found at high temperature, corresponding to the breaking of the $Z(3)$ center symmetry. The phase transition weakens with decreasing quark mass until it disappears at a critical point. This is exactly what is also found in Monte Carlo simulations of full QCD [9, 10]. However, contrary to full QCD, the effective theory can also be applied to

finite chemical potential [8]. For heavy quarks, the first-order deconfinement transition also weakens with chemical potential ending in a critical point, whose location depends on the quark mass, Fig. 1. The same qualitative behaviour is also found by continuum Polyakov loop model studies [11, 12].

2.2. The baryon onset transition

More difficult to address is the cold and dense region, since the sign problem grows exponentially with μ/T . Here we switch to analytic methods. It is instructive to first consider the strong coupling ($\beta = 0$) limit with a static quark determinant. In this case the partition function can be solved analytically. A low temperature, mesonic contributions are exponentially suppressed by chemical potential and for $N_f = 1$ we have [13, 6]

$$Z(\beta = 0) \xrightarrow{T \rightarrow 0} z_0^V \quad \text{with} \quad z_0 = 1 + 4h_1^3 + h_1^6. \quad (5)$$

Note that this corresponds to a free baryon gas with two species. With one quark flavour only, there are no nucleons and the first prefactor indicates a spin 3/2 quadruplet of Δ 's whereas the second term is a spin 0 six quark state or di-baryon. The quark number density is now easily evaluated

$$n = \frac{T}{V} \frac{\partial}{\partial \mu} \ln Z = \frac{1}{a^3} \frac{4N_c h_1^{N_c} + 2N_c h_1^{2N_c}}{1 + 4h_1^{N_c} + h_1^{2N_c}}, \quad \lim_{T \rightarrow 0} a^3 n = \begin{cases} 0, & \mu < m \\ 2N_c, & \mu > m \end{cases}. \quad (6)$$

At zero temperature this is a step function, which reflects the ‘‘silver blaze’’ property of QCD, i.e. the fact that the baryon number stays zero for small μ even though the partition function explicitly depends on it [14]. Once the baryon chemical potential $\mu_B = 3\mu$ is large enough to make a baryon ($m_B = 3m$ in the static strong coupling limit), a discontinuous phase transition to a saturated baryon crystal takes place. Note that saturation density here is $2N_c$ quarks per flavour and lattice site and reflects the Pauli principle. This discretisation effect has to disappear in the continuum limit.

In the case of two flavours the corresponding expression reads [6]

$$z_0 = (1 + 4h_d^3 + h_d^6) + (6h_d^2 + 4h_d^5)h_u + (6h_d + 10h_d^4)h_u^2 + (4 + 20h_d^3)h_u^3 + 4h_d^6 h_u^3 + (10h_d^2 + 6h_d^5)h_u^4 + (4h_d + 6h_d^4)h_u^5 + (1 + 4h_d^3 + h_d^6)h_u^6, \quad (7)$$

where we have separate h_1 couplings for the u - and d -quarks. Now we identify also the spin 1/2 nucleons and several other baryonic multi-quark states with their correct spin degeneracy. Remarkably, the spin-flavour-structure of the QCD baryons is obtained in this simple limit!

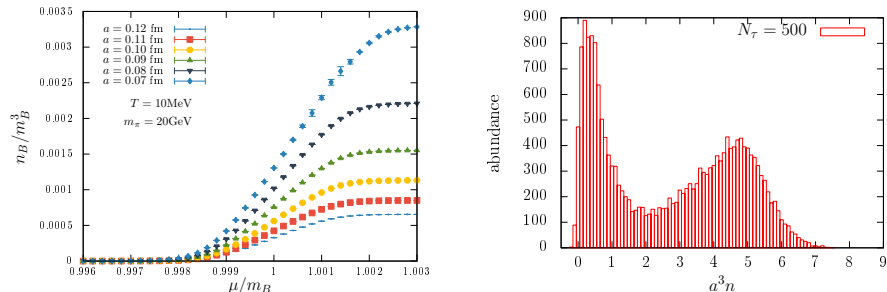


Fig. 2. Left: Baryon number density for heavy quarks, various lattice spacings [8]. Right: Baryon number distribution at onset for low T and light quarks: first-order transition.

When corrections are added, the step function gets smoothed, as shown in Fig. 2 (left) in a calculation through orders $\kappa^8 u^5$ for various lattice spacings. As expected, the saturation level moves towards infinity as the continuum is approached. Note however, that this makes continuum extrapolations at growing chemical potential formidably difficult to control. An important observation is that the onset transition happens already before $\mu_B = m_B$. This is also expected for the physical nuclear liquid gas transition and is partly due to temperature and partly to an attractive interaction between baryons. The binding energy per baryon in units of the baryon mass can at low temperatures be extracted from (here $N_f = 1$ [6])

$$\epsilon = \frac{e - n_B m_B}{n_B m_B} = -\frac{4}{3} \frac{1}{a^3 n_B} \left(\frac{6h_1^3 + 3h_1^6}{z_0} \right)^2 \kappa^2 + \dots \quad (8)$$

In the static limit this vanishes, for dynamical quarks it slowly grows with decreasing quark mass. This is also the reason why the onset in Fig. 2 (left) is a smooth crossover: $T_c \sim \epsilon$ is exponentially small for heavy quarks. For light quarks (larger κ) the expansion does not converge, but simulations clearly show a two-peak structure of baryon number at low temperatures, signalling a first-order onset transition, Fig. 2 (right). Thus, all qualitative features of the nuclear liquid gas transition are contained in the effective theory and thus have been identified from QCD directly.

3. QCD at large N_c

Considering QCD with a large number of colours has a long history, with the initial hope to develop an expansion scheme that also works for hadronic physics. Here we only summarise the most essential features established in

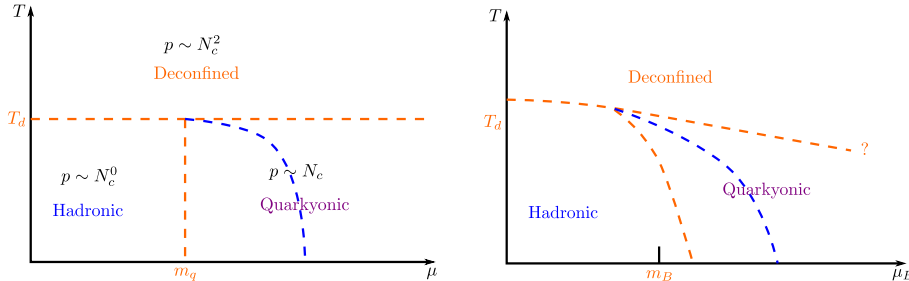


Fig. 3. Phase diagram in the limit of large N_c (left) and possible consequences for $N_c = 3$ (right) according to [3]. The blue line indicates the chiral transition.

the early works [15, 16]. The large N_c limit of $SU(N_c)$ -QCD is defined by

$$N_c \rightarrow \infty \quad \text{with} \quad g^2 N_c = \text{const.} \quad (9)$$

In this case the theory has the following properties:

- Quark loops in Feynman diagrams are suppressed by N_c^{-1}
- Non-planar Feynman diagrams are suppressed by N_c^{-2}
- Meson masses are $\sim \Lambda_{QCD}$
- Mesons are free; the leading corrections are cubic interactions $\sim N_c^{-1/2}$ and quartic interactions $\sim N_c^{-1}$
- Baryons consist of N_c quarks, baryon masses are $\sim N_c \Lambda_{QCD}$
- Baryon interactions are $\sim N_c$

Using this, the authors of [3] conjectured the phase diagram of QCD at large N_c to look like Fig. 3 (left). At large N_c , the influence of fermions on the deconfinement transition is suppressed, which therefore extends horizontally as a first-order transition into the chemical potential plane. In the deconfined phase, perturbation theory is valid and the pressure scales as $p \sim N_c^2$. At low T and μ , the hadron resonance gas is valid, the pressure is exponentially suppressed by hadron masses and scales as $p \sim N_c^0$. At large μ and low T perturbation theory predicts quark matter scaling like $p \sim N_c$. The conjecture of [3] is that this regime reaches all the way down to $\mu \sim m_q$, where one expects baryon matter. The differences in scaling behaviour require non-analytic phase transitions between the three different regimes. Since matter in the cold and dense regime has both baryonic (towards its left boundary) and quark-like (at asymptotic densities) features,

	κ^0	κ^2	κ^4
$h_1 < 1$			
$a^4 p$	$\sim \frac{1}{6N_\tau} N_c^3 h_1^{N_c}$	$\sim -\frac{1}{48} N_c^7 h_1^{2N_c}$	$\sim \frac{3N_\tau \kappa^4}{800} N_c^8 h_1^{2N_c}$
$a^3 n_B$	$\sim \frac{1}{6} N_c^3 h_1^{N_c}$	$\sim -\frac{N_\tau}{24} N_c^7 h_1^{2N_c}$	$\sim \frac{(9N_\tau+1)N_\tau}{1200} N_c^8 h_1^{2N_c}$
ϵ	0	$\sim -\frac{1}{4} N_c^3 h_1^{N_c}$	
$h_1 > 1$			
$a^4 p$	$\sim \frac{4 \ln(h_1)}{N_\tau} N_c$	$\sim -12 N_c$	$\sim 198 N_c$
$a^3 n_B$	~ 4	$\sim -N_\tau \frac{N_c^4}{h_1^{N_c}}$	$\sim -\frac{(59N_\tau-19)N_\tau}{20} \frac{N_c^5}{h_1^{N_c}}$
ϵ	0	~ -6	

Table 1. Large N_c behaviour of the thermodynamic functions and the interaction energy per baryon, order by order in the hopping expansion, on both sides of the onset transition for $N_f = 2$.

it was termed “quarkyonic”. A simple picture arises at low temperatures in momentum space, where fermions form a Fermi sphere, which constitutes the ground state. Excitations of order Λ_{QCD} relative to the Fermi sphere are then expected to be baryonic, whereas excitations $\gg \Lambda_{\text{QCD}}$ should be quark-like in nature. Thus in momentum space a shell structure is expected [3], with an inner quark sphere surrounded by a baryonic shell of thickness $\sim \Lambda_{\text{QCD}}$. The size of the entire and inner sphere is thus governed by μ . A qualitative discussion of the (T, μ, N_c) phase diagram is also given in [17], and there are speculations about quarkyonic physics in heavy-ion collisions [18] and neutron stars [19]. For an introduction, see [20].

3.1. The liquid gas transition for general N_c

Within our analytic approach to lattice QCD, we can now employ the effective lattice theory to study the behaviour of the baryon onset transition as a function of increasing N_c [21]. It should be stressed that we are *not* doing any expansion in N_c^{-1} , so our results apply to any N_c small and large. On the other hand, we do an expansion in the inverse gauge coupling and quark mass, whose implications we will discuss below.

We begin by looking at the changes to the partition function in the static strong coupling limit, Eq. (5), which now reads

$$z_0 = 1 + (N_c + 1)h_1^{N_c} + h_1^{2N_c}. \quad (10)$$

The modified prefactor indicates a different spin degeneracy of the baryon, which naturally depends on the number of quarks that it is made of.

Computing corrections in the hopping expansion, we obtain the coefficients for the pressure and baryon number shown in Table 1. Remarkably,

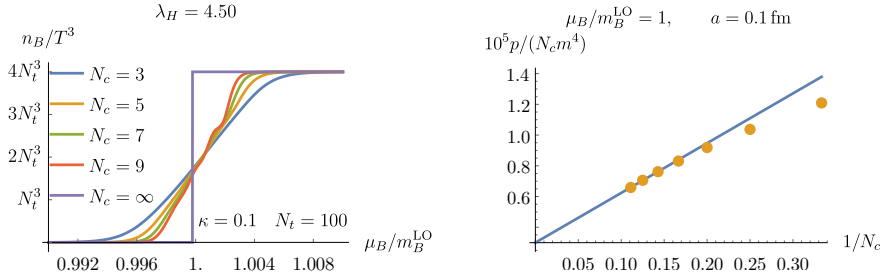


Fig. 4. Left: Onset transition for different values of N_c . Right: Pressure scaling as $p \sim N_c(1 + \text{const. } N_c^{-1} + \dots)$ [21].

for $h_1 > 1$, i.e., to the right of the onset transition, the coefficients of all three computed orders are proportional to N_c , corresponding to part of the definition of quarkyonic matter. For the LO coefficient this is trivial and given by the lattice saturation in terms of quark degrees of freedom. However, the next two terms do not contribute to lattice saturation, but to the description of the physical baryon density which, right at the onset transition, is composed of baryons, not quarks. The fact that these coefficients scale as N_c is non-trivial and suggestive for this to be a feature to all orders. Note also that the binding energy per baryon is N_c^0 as expected [3, 16]. On the other hand, for $h_1 < 1$ the contributions to the thermodynamic functions go as powers of h_1 , which vanish exponentially with $T \rightarrow 0$. Thus the silver blaze feature is amplified as N_c increases, while for $h_1 > 1$ the baryon density gets amplified with growing N_c . This steepens the onset transition with growing N_c , to ultimately always produce a first-order transition.

However, the results in the table were obtained in the strong coupling limit $\beta = 0$ and hence do *not* yet correspond to the ‘t Hooft limit Eq. (9), for which g^2 needs to be adjusted. Thus, including gauge corrections is mandatory. Fig. 4 shows the steepening of the onset transition and the pressure with gauge corrections included. It is remarkable that the pressure scaling with N_c needs only a leading correction to describe the behaviour almost down to $N_c = 3$. Finally, if we are interested in continuum physics, the ordering of limits matters, as already observed in [22]. The fact that for large N_c the baryon density jumps to the lattice saturation density, an artefact of the discretisation, indicates that we have to take the continuum limit first and only then $N_c \rightarrow \infty$. Unfortunately, this prohibits a demonstration of the large N_c behaviour in the continuum, because an exploding number of orders in the expansions would be required to actually take the limits. What is possible at present is to show that both qualitative features, i.e. the steepening of the transition with N_c and $p \sim N_c$ beyond onset, are stable when the lattice is made gradually finer before increasing N_c [21].

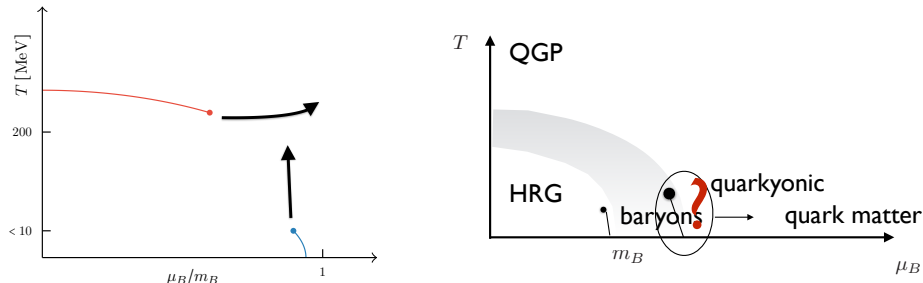


Fig. 5. Left: Smooth change of the transition lines for heavy QCD with growing N_c . Right: The features of the physical QCD phase diagram seen on the lattice.

4. Conclusions

We have studied the onset transition to baryon matter for general number of colours N_c with an effective lattice theory for heavy quarks, which is derived from full lattice QCD by analytic character and hopping expansion methods. The onset transition becomes more strongly first-order with increasing N_c , which implies increasing T_c for its endpoint as well, cf. Fig. 5 (left). Since the deconfinement transition is known to “straighten” with growing N_c , we observe how the phase diagram of QCD with heavy quarks gradually evolves towards the conjectured rectangular shape in the large N_c limit, Fig. 3 (left). We also confirm the pressure beyond the onset transition to scale as $p \sim N_c$ in that limit. If this finding generalises to all orders in the hopping expansion, then it also holds for light quarks and cold and dense QCD is consistent with quarkyonic matter as formally defined in [3].

What are the consequences for physical QCD? For $N_c = 3$, there is no separate phase transition to quarkyonic matter as in Fig. 3 (right), that role is played by the nuclear liquid gas transition, which terminates at $T_c \sim 16$ MeV. There is so far no lattice evidence for the other transition lines either, which might be crossovers. Right after onset there are then baryons only, which is consistent with the shell picture of quarkyonic matter and similar to the finite temperature crossover region still being mostly hadronic [23]. This is indicated by the shaded area in Fig. 5 (right). With increasing density one would then expect the inner sphere of quark matter to form, allowing for a possibly smooth transition to predominantly quark matter at large densities, similar to the smooth transition to quark gluon plasma in the temperature direction. A separate study with light quarks is needed to see whether or not there is in addition a chiral transition.

Acknowledgments: The authors acknowledge support by the Deutsche Forschungsgemeinschaft (DFG) through the grant CRC-TR 211 “Strong-interaction matter under extreme conditions”.

REFERENCES

- [1] C. Ratti, PoS **LATTICE2018** (2019), 004
- [2] O. Philipsen, PoS **LATTICE2019** (2019), 273 [arXiv:1912.04827 [hep-lat]].
- [3] L. McLerran and R. D. Pisarski, Nucl. Phys. A **796** (2007) 83 [arXiv:0706.2191 [hep-ph]].
- [4] J. Langelage, S. Lottini and O. Philipsen, JHEP **1102**, 057 (2011) [JHEP **1107**, 014 (2011)] [arXiv:1010.0951 [hep-lat]].
- [5] M. Fromm, J. Langelage, S. Lottini and O. Philipsen, JHEP **1201** (2012) 042 [arXiv:1111.4953 [hep-lat]].
- [6] J. Langelage, M. Neuman and O. Philipsen, JHEP **1409**, 131 (2014) [arXiv:1403.4162 [hep-lat]].
- [7] J. Kim, A. Q. Pham, O. Philipsen and J. Scheunert, JHEP **10** (2020), 051 [arXiv:2007.04187 [hep-lat]].
- [8] J. Glesaaen, M. Neuman and O. Philipsen, JHEP **1603**, 100 (2016) [arXiv:1512.05195 [hep-lat]].
- [9] S. Ejiri *et al.* [WHOT-QCD], Phys. Rev. D **101** (2020) no.5, 054505 [arXiv:1912.10500 [hep-lat]].
- [10] F. Cuteri, O. Philipsen, A. Schön and A. Sciarra, [arXiv:2009.14033 [hep-lat]].
- [11] P. M. Lo, B. Friman and K. Redlich, Phys. Rev. D **90**, no. 7, 074035 (2014) [arXiv:1406.4050 [hep-ph]].
- [12] C. S. Fischer, J. Luecker and J. M. Pawłowski, Phys. Rev. D **91**, no. 1, 014024 (2015) [arXiv:1409.8462 [hep-ph]].
- [13] M. Fromm, J. Langelage, S. Lottini, M. Neuman and O. Philipsen, Phys. Rev. Lett. **110** no. 12, 122001 (2013) [arXiv:1207.3005 [hep-lat]].
- [14] T. D. Cohen, Phys. Rev. Lett. **91**, 222001 (2003) [hep-ph/0307089].
- [15] G. 't Hooft, Nucl. Phys. B **72** (1974) 461.
- [16] E. Witten, Nucl. Phys. B **160** (1979) 57.
- [17] G. Torrieri, S. Lottini, I. Mishustin and P. Nicolini, Acta Phys. Polon. Supp. **5** (2012) 897 [arXiv:1110.6219 [nucl-th]].
- [18] A. Andronic *et al.*, Nucl. Phys. A **837** (2010), 65 [arXiv:0911.4806 [hep-ph]].
- [19] L. McLerran and S. Reddy, Phys. Rev. Lett. **122** (2019) no.12, 122701 [arXiv:1811.12503 [nucl-th]].
- [20] L. McLerran, Acta Phys. Polon. B **51** (2020), 1067-1077
- [21] O. Philipsen and J. Scheunert, JHEP **11** (2019), 022 [arXiv:1908.03136 [hep-lat]].
- [22] D. J. Gross and E. Witten, Phys. Rev. D **21** (1980) 446.
- [23] C. Rohrhofer *et al.*, Phys. Rev. D **100** (2019) no.1, 014502 [arXiv:1902.03191 [hep-lat]].